TSF0023

Dynamic behavior of vortices rolled up from a heaving elastic airfoil by a FSI simulation

Masaki Fuchiwaki[1, *], and Aphaiwong Junchangpood [2]

1 Kyushu Institute of Technology, 680-4 Kawazu, Iizuka, 820-8502, Japan
2 King Mongkut's University of North Bangkok, 1518 Pibulsongkram Road Bangsue, Bangkok, 10800, Thailand

* Corresponding Author: futiwaki@mse.kyutech.ac.jp

Abstract. The flow field around an unsteady airfoil is a common type of unsteady flow. In recent years, the flow field around an elastic moving body has been attracted attention. The flow around an elastic body is treated as a coupled problem between the fluid and structure and a series of phenomena, motions, structural deformations and the generation/growth/ development of vortices are repeated continuously. The studies on the flow filed around the elastic moving body have also carried out with experimental and numerical approaches. The macro scale vortex structure and the dynamic forces acting on the elastic moving airfoil have been understood. However, the impact of elastic deformation effects on the vortices generated in the vicinity of the wall and the dynamic behaviors of the micro scale vortices have not been clarified sufficiently. In this study, the dynamic behaviors of the leading edge vortex and the vorticity in the vicinity of the wall of the heaving elastic airfoil in a separation region are investigated by FSI simulation using ANSYS 16.1/ANSYS CFX 16.1 and these behaviors is related with the characteristics of the dynamic lift. The dynamic lift acting on the elastic airfoil becomes higher than that on the rigid airfoil due to the boundary layer formed by the elastic deformation of the wall in addition to the small effective angle of attack.

1. Introduction

The flow field around a moving airfoil is one of the typical unsteady flow and many studies on the flow field around the moving airfoil have been carried out with experimental and numerical approaches. Especially, not only the dynamic behavior of the leading edge vortex and wake structure of moving airfoils, such as a pitching airfoil, a heaving airfoil, and a combination airfoil with pitching and heaving motions, but also their dynamic lift and thrust characteristics have been already reported [1,2,3,4,5]. We have also qualitatively and quantitatively characterized the vortex structures in the wake of a rigid airfoil with pitching motion [6], heaving motion [7] and combination motions [8]. Furthermore, dynamic thrust on the airfoil was measured, and the relationship between the vortex structures in the wake of the moving airfoil and the dynamic thrust properties have also been clarified. In recent years, the flow field around an elastic moving body has been attracted attention from the viewpoint of the insect flights, the aquatic animal swimming, the development of MAVs and the application to turbomachinery. The flow field around the elastic body is treated as a coupled problem between the fluid and structure (fluid structure interaction, FSI), and a series of phenomena, motions, structural deformations and the generation/growth/development of vortices are repeated continuously. Many studies on the flow filed around the elastic moving body have also carried out. Heathcote et al. [9,10] visualized wakes of a heaving airfoil with a thin plate that elastically deforms on its trailing
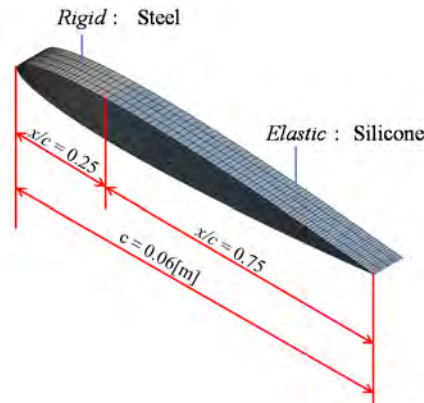
Figure 1. Rigid and elastic parts of the elastic airfoil and numerical mesh for structure analysis.

edge, measured dynamic forces, and clarified the influence of the thin plate's elasticity on the flow field and the thrust properties. Furthermore, they [11] measured the thrust acting on the elastic airfoil, which deforms elastically in the span direction, and also performed particle image velocimetry (PIV) measurements. We also carried out the PIV measurement in the wake of an elastic heaving airfoil and clarified the relationship between the characteristics of dynamic thrust acting on a heaving elastic airfoil and its wake structure [12]. Kurinami et al. [13] reported that the dynamic thrust acting on a heaving airfoil depends strongly on the Strouhal number, which is proportional to the maximum amplitude at the trailing edge of the airfoil. Moreover, the investigation of the flow field around the elastic moving airfoil is approached by the numerical simulation. We performed fluid structural interaction simulation of the flow field around the elastic heaving airfoil using ANSYS/ANSYS-CFX and clarified the relationship between three key parameters, Strouhal number St, Reynolds number Re and bending stiffness K and is to elucidate the nature of the dynamic forces acting on an elastic airfoil as a function of these three dimensionless parameters. By defining the new quantity St^2/K, we showed that the characteristic of dynamic forces depends on the ratio St^2/K [14]. The macro scale vortex structure and the dynamic forces acting on the elastic moving airfoil have been understood. However, the impact of elastic deformation effects on the vortices generated in the vicinity of the wall and the dynamic behaviors of the micro scale vortices have not been clarified sufficiently.

The objectives of this study is to investigate the dynamic behavior of the leading edge vortex and the vorticity in the vicinity of the wall of the heaving elastic airfoil in a separation region by FSI simulation using ANSYS 16.1/ANSYS CFX 16.1. Moreover, these behaviors is related with the characteristics of the dynamic lift and we clarify the impact of elastic deformation effects on the flow field around the heaving elastic airfoil.

2. Fluid structure interaction simulation

2.1. Airfoils

The rigid and elastic airfoils used in our numerical simulation are a NACA0010 airfoil. The chord length c of the airfoil is 60 [mm] and the Reynolds number based on the chord length is 4,000. In the elastic airfoil consists of a rigid part and an elastic part. The first quarter part is the rigid and the rear other part is the elastic, as shown in Fig. 1. The Young module and the density of the elastic part is $E = 0.06$ [MPa] and $\rho = 1143$ [kg/m^3]. The heaving motion of Eq. (1) was applied to the quarter chord axis of the airfoil. The Strouhal number is given by Eq. (s) as a function of the maximum trailing edge amplitude and was 0.3 in this study. The flapping frequency, the main flow velocity and the heaving amplitude were 0.833 [Hz], 0.067 [m/s] and 0.0012 [m], respectively.
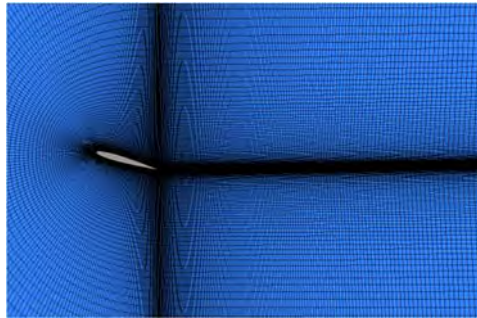
$$y = a\sin(2\pi f t) \qquad (1)$$

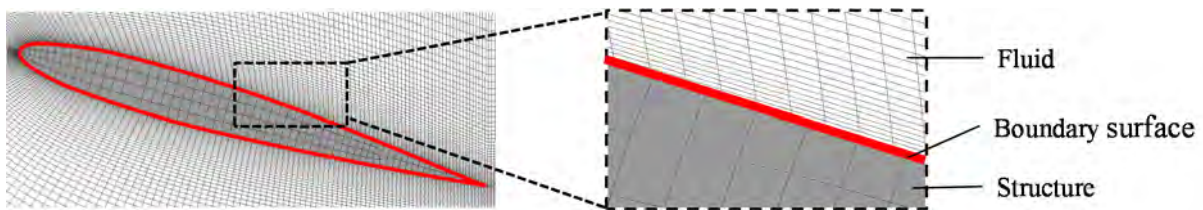**Figure 2.** Numerical mesh for flow analysis.

Figure 3. Boundary surface between fluid and structure domains for fluid structure interaction simulation.

$$St = \frac{2af}{V_0} \qquad (2)$$

2.2. Fluid structure structure interaction simulation

The fluid structure interaction simulation was performed by using ANSYS16.1 and ANSYS-CFX16.1. For the fluid, the governing equations are the continuity and the Navier-Stokes equations given by Eqs. (3) and (4), respectively, and the finite volume method (FVM) was used for discretization. For the structural part, the governing equations are the constitutive equations given by Eq. (5), and the finite element method (FEM) was used for discretization. Figures 2 and 1 show the numerical mesh on the fluid and structure parts, respectively. The numbers of the computational grids for the fluid and structure regions are 280,000 and 5,000, respectively. The height of the first lattice point of the fluid is approximately 0.002% of the chord length c and the turbulence model was k-ω.

In our numerical simulation, the interaction between a fluid and a structure is considered for a bi-directional coupling simulation, as shown in Fig. 3. We use a decoupled solver referred to as the weak coupled method, for which the governing equations of the fluid and structural regions are calculated independently. Although this method has problems with respect to the calculation time, convergence, and mapping of the interface data, the governing equations are calculated precisely. Therefore, data transfer of physical quantities related to the fluid structure interface can be transferred adequately. As a result, actual phenomena related to the fluid and structural regions can be treated strictly.

$$\nabla \bullet U = 0 \qquad (3)$$

$$\rho \frac{\partial U}{\partial t} + U \bullet \nabla U = -\nabla P + \mu \nabla^2 U \qquad (4)$$

$$[M]\ddot{X} + [C]\dot{X} + [K]X = F \qquad (5)$$

3. Results and discussion

Figure 4 shows the time histories of the dynamic lift acting on the rigid and elastic heaving airfoils. Red and blue lines show the result of the rigid and elastic airfoils, respectively, and the black dash line shows the heaving amplitude.
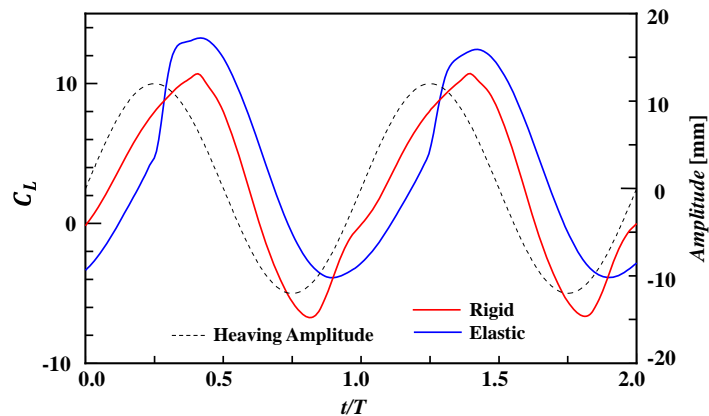
Figure 4. Time histories of dynamic lift acting on heaving airfoils and their heaving amplitudes

There is a phase difference between the dynamic lift acting on rigid and elastic airfoils and the heaving amplitude. Moreover, the dynamic lift acting on the elastic airofil has a phase difference for that in the rigid airfoil. It is thought that the phase difference between the elastic and rigid airfoils occurs due to the effective angle of attack. The effective angle of attack of the elastic airfoil is smaller than that of the rigid airfoil due to the elastic deformation of the rear part of the elastic airfoil. As a result, the dynamic behaviour of the leading edge vortex of the elastic airfoil delays than that of the rigid airfoil. Finally, the dynamic lift acting on the elastic airfoil delay than that on the rigid airfoil. Furthermore, the dynamic lift acting on the elastic airfoil is larger than that on the rigid airfoil. Especially, the dynamic lift increases rapidly at $0.250 < t/T < 0.333$ and the maximum dynamic lift of the elastic airfoil at $t/T = 0.42$ is 1.24 times as large as that of the rigid airfoil. In this study, the authors attracted attention the phase difference of the dynamic lift between the rigid and elastic airfoils and the large dynamic lift of the elastic airfoil.

Figure 5(a) and (b) shows the vorticity distributions around the leading edge of the heaving rigid and elastic airfoils, respectively, at $t/T = 0.333$, 0.417 and 0.500. The blue and red indicate vorticity rotation in the clockwise and counterclockwise directions, respectively. $t/T = 0.5$ correspond to the centers of the heaving motion from the top dead position to the bottom dead position.

The leading edge vortex rolled up of the rigid airfoil at $t/T = 0.333$, On the other hand, the leading edge vortex did not roll up and the separation did not occur at $t/T = 0.333$ of the elastic airfoil. At $t/T = 0.417$, the leading edge vortex rolled up from the leading edge of the elastic airfoil. The leading edge vortex on the rigid airfoil separates completely from the suction surface at $t/T = 0.500$ however the leading edge vortex on the elastic airfoil still attaches on the suction surface. Morover, the maximum vorticity of the leading edge vortex is higher than that of the rigid airfoil at $t/T = 0.500$. That is, the growth of the leading edge vortex of the elastic airfoil delays than that of the rigid airfoil. Actually, the effective angle of attack of the elastic airfoil is smaller than that of the rigid airfoil. Based on these results, we found that the dynamic behaviour of the dynamic lift acting on the elastic airfoil delays than that of the rigid airfoil and the maximum dynamic lift acting on the elastic airfoil is higher than that of the rigid airfoil.

Next, we attracted attention about the dynamic behaviour of the vorticity on the rear part of the elastic airfoil. Figure 6(a) and (b) shows the vorticity distributions in the vicinity of the wall of the heaving rigid and elastic airfoils, respectively, at $t/T = 0.417$.

The vorticity with clockwise rotation grows in the vicinity of the wall of the elastic airfoil. That is, the separation does not occur in the vicinity of the wall of the elastic airfoil. The vorticity with the clockwise rotation existed from $t/T = 0.417$ to 0.500. In the rigid airfoil, on the other hand, the vorticity with counterclockwise rotation exist in the vicinity of the wall. it is found that the back flow from the trailing edge to the leading edge exist in the vicinity of the wall of the rigid airfoil.
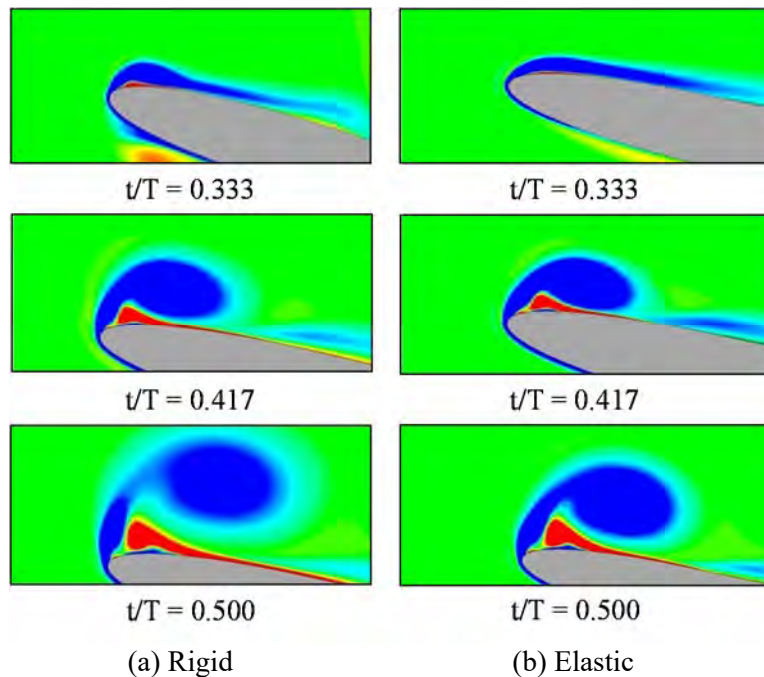
(a) Rigid   (b) Elastic

Figure 5. Dynamic behaviors of a leading edge vortex on heaving airfoils
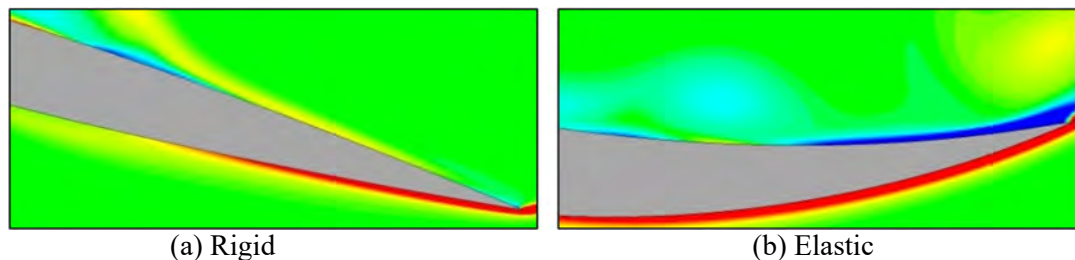

(a) Rigid   (b) Elastic

Figure 6. Dynamic behaviors of vorticity in vicinity of wall on heaving airfoils at t/T =0.417

In order to investigate the details of the flow field in the vicinity of the wall, we measured the velocity profile in the vicinity of the wall of the heaving airfoils. Figures 7(a) and (b) show the measurement points of the velocity profile of the rigid and elastic airfoils, respectively. The measurement points are x/c = 0.4, 0.5, 0.6, 0.7, 0.8 and 0.9. The velocity profile indicates the velocity vector of the vertical cross section to the plane of the wall and was measured from the wall to height of $0.06c$. Figures 8(a) and (b) show the velocity vectors in the vicinity of the wall of the heaving airfoils at t/T = 0.417.

    In the velocity profile on the rigid airfoil from x/c = 0.5 to 0.7, the velocity is low in the vicinity of the wall. That is, the separation occurs completely on the rear part of the rigid airfoil. In the elastic airfoil, on the other hand, the boundary layer is formed at all measurement points. Especially, at the x/c = 0.7 having large elastic deformation, the boundary layer is formed clearly and the velocity is high. That is, the boundary layer is formed by the elastic deformation of the wall in large elastic deformation parts and the separation is controlled finally. It is expected that the vorticity with clockwise rotation in the vicinity of the wall on the elastic airfoil, as shown in Fig. 6(b), means the boundary layer. Moreover, it is thought that the pressure on the rear part of the elastic airfoil decreases by the boundary layer on the wall and the dynamic lift acting on the elastic airfoil increases, as shown in Fig. 4. Based on these results, we thought that the dynamic lift acting on the elastic airfoil become higher than that on the rigid airfoil due to the boundary layer formed by the elastic deformation of the wall in addition to the small effective angle of attack.
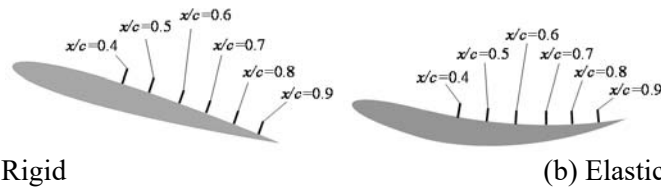
(a) Rigid   (b) Elastic

Figure 7. Measurement points of the velocity profile of the heaving airfoils at t/T =0.417
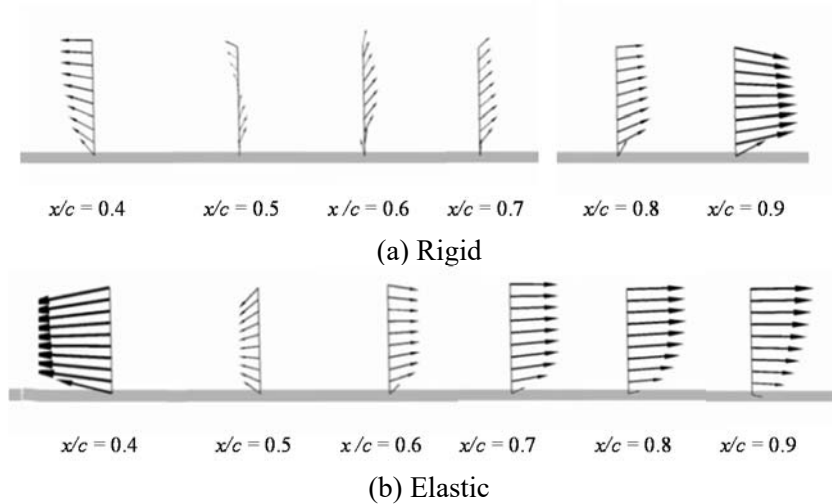

(a) Rigid

(b) Elastic

Figure 8. Velocity profile in vicinity of wall of the heaving airfoils at t/T =0.417

4. Conclusion

The dynamic behaviors of the leading edge vortex and the vorticity in the vicinity of the wall of the heaving elastic airfoil in a separation region are investigated by FSI simulation using ANSYS 16.1/ANSYS CFX 16.1 and these behaviors is related with the characteristics of the dynamic lift.

The dynamic lift acting on the elastic airfoil is larger than that on the rigid airfoil and the dynamic behaviour of the dynamic lift acting on the elastic airfoil delay than that on the rigid airfoil. The effective angle of attack of the elastic airfoil becomes smaller than that of the rigid airfoil and the maximum vorticity of the leading edge vortex is higher. Moreover, the boundary layer is formed by the elastic deformation of the wall in large elastic deformation parts and the separation is controlled. Based on these reasons, the dynamic lift acting on the elastic airfoil is larger and is delayed.

References

[1] Platzer M F and Jones K D, 2008, *AIAA J.*, **46**, 9, 2136
[2] Jones K D, Dohring C M and Platzer M F, 1998, *AIAA J.* **36**, 7, 1240
[3] Lai J C S and Platzer M F, 1999, *AIAA J.*, **37**, 12, 1529
[4] Ramamurti R and Sandberg W, 2001, *AIAA J.*, **39**, 2, 253
[5] Triantayllou G S and Grosenbaugh M A, 1993, *J. Fluid Stru.*, **7**, 205
[6] Fuchiwaki M and Tanaka K, 2000, *JSME Int. J.*, B, **43**, 3, 443
[7] Fuchiwaki M and Tanaka K, 2005, *Proc. ASME Fluid Eng. Sum. Meet.*, FEDSM2005-77473
[8] Fuchiwaki M, Tanaka K and Nakashima M, 2007, *Proc. ASME Fluid Eng. Sum. Meet.,* FEDSM2007-37222.
[9] Heathcote S, Martin D and Gursul I, 2004, *AIAA J.*, **42**, 11, 2196
[10] Heathcote S and Gursul I, 2007, *AIAA J.*, **45**, 5, 1066
[11] Heathcote S, Wang Z and Gursul I, 2004 *J. Fluid Stru.*, **24**, 2, 183
[12] Fuchiwaki M, Kurinami T and Tanaka K, 2009, *J.Fluid Sci Tech.*, **4**, 2, 391
[13] Kurinami T, Fuchiwaki M and Tanaka K, 2011, *J.Fluid Sci Tech.*, **6**, 4, 562
[14] Fuchiwaki M, Nagata T and Tanaka K, 2014, *Proc. ASME Fluid Eng. Sum. Meet.,* FEDSM2014-21302